

# Helicon Source for Ion Propulsion

**Francis F. Chen**

*Electrical Engineering Department, University of California, Los Angeles, California, U.S.A.;*

*ffchen@ee.ucla.edu; www.ee.ucla.edu/~ffchen*

## Keywords

Space propulsion, electric thruster, helicon source, radiofrequency plasma

## Abstract

Electric thrusters are usually in one of two forms: gridded ion thrusters or Hall thrusters. Each of these accelerates ions and requires an injector of electrons to neutralize the ion beam. Ambipolar thrusters eject neutralized plasmas with equal numbers of ions and electrons. Helicon thrusters are a new type being developed which utilize both the high ionization efficiency of magnetized helicon discharges to produce dense plasma and the properties of an expanding magnetic field to accelerate the ions.

## Introduction

Propulsion of spacecraft [1] requires the ejection of mass at an exhaust velocity  $v_{ex}$ , assumed to be positive and constant here. The propellant, usually xenon, has mass  $m_p$  and is consumed in the process. The thrust  $T$  (a forward force measured in newtons) is the negative of the change of the propellant's backward momentum  $m_p v_{ex}$ :

$$T = -v_{ex} (dm_p / dt). \quad (1)$$

How this compares with the force of gravity is quantified by the specific impulse  $I_{sp}$ , defined by

$$I_{sp} \equiv v_{ex} / g = -\frac{T}{g(dm_p / dt)}, \quad (2)$$

where  $g$  is the acceleration of gravity, of magnitude  $9.8 \text{ m/sec}^2$ . Note that  $I_{sp}$  has units of seconds. If one drops a rock from a height, it will accelerate to a velocity  $v_{ex}$  in  $I_{sp}$  seconds.

The basic principles of space propulsion will serve as a background for helicon thrusters. Let  $M$  be the total mass of the load consisting of the intrinsic spacecraft mass  $m_s$  plus the decreasing propellant mass  $m_p$ :

$$M(t) = m_s + m_p(t) \quad (3)$$

In the frame of the spacecraft, its velocity  $v$  is zero, and its acceleration  $dv/dt$  is positive, The thrust  $T$  is the negative of the rate of change of exhaust momentum:

$$T = -\frac{d}{dt}(m_p v_{ex}) = -v_{ex} \frac{dM}{dt}. \quad (4)$$

The thrust causes the spacecraft to accelerate

$$T = \frac{d}{dt}(Mv) = M \frac{dv}{dt}. \quad (5)$$

Thus,

$$\frac{dv}{dt} = -v_{ex} \frac{1}{M} \left( \frac{dM}{dt} \right) = -v_{ex} \left[ \frac{d(\ln M)}{dt} \right] \quad (6)$$

Integration from the initial velocity  $v_i$  to the final one  $v_f$  as  $m_p$  goes from  $m_{p0}$  to 0 gives

$$\int_{v_i}^{v_f} v dt \equiv \Delta v = -v_{ex} \int_{M_i}^{M_f} \frac{d(\ln M)}{dt} dt = -v_{ex} \ln \left( \frac{m_s}{m_s + m_{p0}} \right). \quad (7)$$

The mass of propellant needed for a given  $\Delta v$  is then [1]

$$m_{p0} = m_s \left( e^{\Delta v / v_{ex}} - 1 \right). \quad (8)$$

The amount of propellant needed to accelerate a given mass to a given velocity depends exponentially on the exhaust velocity  $v_{ex}$ . Helicon sources are of interest because of the large exhaust velocity achievable with the “double layer” effect described below.

## Thruster types

Thrusters in current use are mainly of two types: gridded ion thrusters and Hall thrusters. A schematic of a gridded thruster is shown in Fig. 1. A plasma is created by a voltage applied between a cathode and an anode grid. The cathode could be a good electron emitter like lanthanum hexaboride ( $\text{LaB}_6$ ). Electrons are retained and ions are accelerated by grids. The ion beam will not detach from the spacecraft unless it is neutralized, so electron emitters have to be added at the sides to inject electrons into the accelerated ion beam and prevent the spacecraft from charging to a high negative potential. The neutralizers are usually hollow-cathode discharges. The ejected plume of plasma can then be formed by nozzles into an optimal shape. Sputtering limits the lifetime of the grids, but they have been designed to last at least 30,000 hours.

Elements of a Hall thruster are shown in Fig. 2, which is a cross section of a cylindrically symmetric device. A plasma is formed between the coaxial cylinders by applying a high voltage to the anode ring at the left. This voltage accelerates the ions to  $v_{\text{ex}}$ . Holes in the ring also serve as the gas feed, as shown in the upper cross section. Xenon is normally used because of it is an inert, monatomic gas with high mass and low ionization potential. A radial magnetic field is created by coils (not as shown) in order to prevent electrons from following the ions. The electrons instead drift azimuthally with their  $\mathbf{E} \times \mathbf{B}$  drift, forming the Hall current. Here again, electron neutralizers have to be added to neutralize the ejected ion beam. The function of the magnetic field is to prevent the electrons from moving axially and collapsing the anode voltage into a thin sheath at the anode. Hall thrusters have a few intrinsic problems. One is secondary emission of cold electrons from the internal surfaces which can upset the charge balance in the plasma. This can be minimized by coating the surfaces with carbon velvet. A second problem is instability, since many types of instabilities arise when there is a magnetic field (B-field). In spite of these problems, Hall thrusters have been engineered successfully to fly in space.

A new, third type of thruster is the helicon thruster, the subject of this article. In addition to having a high ionization efficiency, helicon thrusters do not require an electron neutralizer, since they can accelerate an entire neutralized plasma.

## Helicon discharges

Helicon discharges are radiofrequency (RF) plasmas in DC B-fields discovered in England in the early 1960s [2] and developed in Australia since 1970 [3] and the United States since 1985 [4]. In initial studies in straight cylinders, helicon discharges attracted interest because they produced unusually high plasma densities at any given RF power. Ionization was at first thought to be caused by Landau damping [4], but this was disproved later [5] as Landau-driven electrons were found but in insufficient numbers. Instead, Shamrai and Taranov [6] proposed that an electron cyclotron wave at the boundary, the so-called Trivelpiece-Gould (TG) mode, did most of the ionization. This was shown to be correct [7], since the TG mode is needed to satisfy all the boundary conditions. Elaborate measurements by Krämer, Aliev, *et al.* [8] showed that the TG modes coupled to the plasma via parametric instabilities. Helicons are complex because they involve both magnetic fields and collisions with neutral atoms. Over 660 papers on helicons had appeared by 2013. Those up to 1997 have been summarized by Boswell [9] and Chen [10].

The DC magnetic field required by helicons, which can be 0.1T or higher, is usually generated by currents in magnetic coils driven by a large DC power supply. In spacecraft, it may be possible to design coils that utilize the currents from solar cells directly. Alternatively, one can use permanent magnets, either in the form of rings [11] or rods [12].

## Double-layer acceleration

In a bounded plasma, electrons are contained by sheath voltages at the walls so that they do not escape with their large thermal velocities, leaving un-neutralized ions behind. Sheaths are thin, ion-rich layers providing Coulomb repulsion of the electrons [Fig. 3]. For the sheath voltage to have the right sign, ions must enter the sheath with at least their acoustic velocity  $c_s$  [Eq. (9)], so that their orbits in the

$$c_s \equiv (KT_e / M_i)^{1/2} \quad (9)$$

sheath are stiff enough to ensure that their density  $n_i$  be larger than the electrons'  $n_e$ . This “Bohm criterion” is slightly modified if the ions are not monoenergetic or singly charged ( $Z = 1$ ). In most plasmas the ions are accelerated to  $c_s$  in a pre-sheath, in which collisions and ionization can occur. In a uniform B-field, this occurs at walls that intercept the B-field. (Transport to walls parallel to  $\mathbf{B}$  is not considered here since it is often anomalous due to instabilities.) In a diverging B-field, however, a pre-sheath is not necessary for accelerating ions to the Bohm speed. This is a consequence of the tendency of electrons to fall into a Maxwellian distribution and follow the Boltzmann equation [Eq. (10)], even across the B-field [13]:

$$n_e = n_0 e^{e(V-V_0)/KT_e} \rightarrow n_0 e^{eV/KT_e} \quad (V_0 = 0, V < 0). \quad (10)$$

where  $n_0$  is the maximum density and  $V_0$  is the potential there, and, for simplicity, is set as 0 here. Here “e” is used for the base of natural logarithms and “e” for the unit of charge. Figure 4 shows the field lines from a helicon tube diverging into a large chamber. A sheath will form at a specific place in the expanded region. The ion energy at the sheath edge,  $\frac{1}{2}M_i c_s^2$ , is  $\frac{1}{2}KT_e$  from Eq. (9). To accelerate ions to this energy, the potential at the sheath edge,  $V_s$ , must be at least  $-\frac{1}{2}KT_e/e$ . Hence, the quasineutral density at the sheath edge,  $n_s$ , is given by Eq. (10) as

$$n_s = n_0 e^{-1/2}. \quad (11)$$

Since magnetic flux is conserved in the expansion from  $r_0$  to  $r$  for each field line, and since electrons are constrained to follow the field lines, the field and density vary with  $r$  as

$$\frac{B}{B_0} = \frac{n}{n_0} = \left(\frac{r_0}{r}\right)^2. \quad (12)$$

The radius at which a sheath forms is then

$$\frac{r_s}{r_0} = \left(\frac{n_0}{n_s}\right)^{1/2} = e^{1/4} = 1.28. \quad (13)$$

Thus, an ion sheath will form at a position where the field lines have increased their distances from the axis by 28%. Since there is no physical boundary there, electrons will be attracted to the ion layer,

forming a “double layer” and preserving quasineutrality. The expanding B-field serves the function of the pre-sheath by creating an electric field as the density drops, according to Eq. (10), and accelerating ions to  $c_s$ , whereupon a sheath must form, whether there is a solid boundary or not [14].

The magnitude of the potential drop at a double layer can be estimated by considering a normal sheath, at which the drop reduces the electron flux to the same value as the ion flux (for  $Z = 1$ ). From Eq. (11), the ion flux is

$$n_s c_s = n_0 e^{-1/2} \left( \frac{KT_e}{M_i} \right)^{1/2}, \quad (14)$$

and the electron flux, in a direction  $+x$ , say, is

$$\frac{1}{2} n_0 \bar{v}_x e^{eV/KT_e} = n_0 \left( \frac{KT_e}{2\pi m} \right)^{1/2} e^{eV/KT_e}. \quad (15)$$

Equating these fluxes yields

$$\frac{eV}{KT_e} = \frac{1}{2} \ln \left( \frac{2\pi m}{eM} \right). \quad (16)$$

The sheath drop is then  $-5.18 T_{eV}$  for argon and  $-5.78 T_{eV}$  for xenon, where  $T_{eV}$  is  $KT_e$  in electron volts.

In theory, ions in a 5-eV plasma could be accelerated to 26 eV in Ar and 29 eV in Xe in a double layer.

The source of energy for the fast ions ultimately comes from what the discharge uses to replenish the tail of the electron distribution. This is explained in detail by Chen [14]. The thrust is applied to the spacecraft by the ion bombardment of the endplate and the  $\mathbf{J} \times \mathbf{B}$  force of the diamagnetic current acting on the radial component of the B-field.

## Experiments

Experiments on helicon double-layer thrusters have been summarized by C. Charles [15, 16]. As one example, M.D. West *et al.* [17] injected the plasma from a helicon double-layer thruster into a large space-simulation chamber. A generic schematic of the device [16] is shown in Fig. 5. A double layer

formed 1–2 cm past the exit of the helicon source. A reversed-field energy analyzer past the double layer showed two peaks, one at the local space potential and the other 16V beyond that, indicative of an ion beam with  $v_{\text{ex}} = 8.7$  km/sec. This gives a specific impulse  $I_{\text{sp}}$  [Eq. (2)] of  $\sim 900$  sec with  $B = .0138$  T,  $p = 53.3$  mPa (0.4 mTorr) of Ar, and 100W of 13.56 MHz power. At lower pressures,  $I_{\text{sp}}$ 's of up to 1500 sec could be achieved. Effective  $I_{\text{sp}}$ 's are higher than this because entrained neutral atoms are also ejected, adding to the thrust [18]. Existing gridded electric thrusters achieve  $I_{\text{sp}}$ 's of the order of 7000 sec, but at much higher power (20 kW) [1].

Direct measurements of the thrust from a helicon source have been made by K. Takahashi and co-workers [19, 20]. A helicon discharge was mounted on a movable cart on wheels, and the magnetic coils were movably suspended from above. The entire apparatus was placed inside a large vacuum chamber. It was confirmed that the gas feed alone did not produce a measurable displacement of the discharge. When the helicon discharge is fired, its motion was detected with a laser. The diamagnetic current of the helicon interacts with the radial current in the magnetic coils, causing them to move also. Careful calibration showed that about half the thrust was used to move the coils. With 800W of RF power, the thrust was measured to be 6 mN, half of which was transmitted to the coils.

To simplify thrusters that require a DC B-field, permanent magnets have been tried. Chen and Torreblanca [21] used ring magnets polarized perpendicular to the axis. The axial B-field of these magnets is strongest inside the hole, but plasma placed there cannot be ejected. Further along the axis the B-field reaches a stagnation point, beyond which a weaker and more uniform field extends to infinity [21]. A thruster with a helicon discharge placed in this remote field is shown in Fig. 6. This device can operate at either 13.56 MHz or 27.12 MHz [22], but breakdown is easier at the higher frequency, which also requires smaller components in the power supply and matching circuit. In experiment, the discharge tube is made of quartz, and the grounded endplate is aluminum sealed with an O-ring. In production, the tube would be ceramic, sealed to a conducting endplate with a metal-to-ceramic braze. The endplate serves the function of reflecting the backward helicon wave to interfere constructively with the forward wave. This condition determines the distance of the antenna from the endplate. The antenna is a three-

turn loop at 13 MHz and a single turn at 27 MHz. To prevent plasma loss to the sidewalls, it is placed close to the exit aperture. Linear permanent magnets can also be used. The configuration designed by Takahashi *et al.* [12] is shown in Fig. 7. High B-fields can be obtained with neodymium (NdFeB) magnets, but experiments show that good results can be obtained with B-fields as low as 6 mT [22]. The temperature limit of Nd magnets can thus be avoided by using more robust types.

The first helicon thruster to be flown in space is likely to be the largest one: the VASIMR (Variable Specific Impulse Magnetoplasma) rocket of astronaut Franklin Chang-Diaz [23]. Being developed for interplanetary travel, this 200-kW rocket starts with a 30-kW helicon discharge, whose ions are then accelerated by 170 kW of ion cyclotron resonance heating in superconducting coils. The ion energy is converted to parallel motion in a diverging B-field. This thruster is planned for testing on the International Space Station. The VASIMR project has spurred research on high-power helicon discharges [24].

## Summary

Helicon thrusters are a new type of spacecraft propulsion device under development which has the potential advantages over gridded ion thrusters and Hall thrusters of higher ionization efficiency and ambipolar exhaust that does not require electron neutralizers. In an expanding magnetic field, helicon discharges automatically form a sheath-like “double layer” in which a sheath drop of order 16 eV can accelerate ions to interesting values of the specific impulse. Use of permanent magnets can lead to smaller and simpler thrusters. Though extensively studied in the laboratory, helicon thrusters have not yet been tested in space.



## References

- [1] Goebel, D. M. and Katz, I. Fundamentals of Electric Propulsion: Ion and Hall Thrusters; JPL Space science and technology series, Jet Propulsion Laboratory, California Institute of Technology, Pasadena, California, 2008.
- [2] Lehane, J.A. and Thonemann, P.C. Experimental study of helicon wave propagation in a gaseous plasma. Proc. Phys. Soc. 1965, 85, 301-
- [3] Boswell, R.W. Plasma production using a standing helicon wave. Phys. Lett. A 1970, 33, 457-
- [4] Chen, F.F. Plasma ionization by helicon waves. Plasma Phys. Control. Fusion 1991, 33, 339-
- [5] Molvik, A.W., Ellingboe, A.R., and Rognlien, T.D. Hot Electron production and wave structure in a helicon plasma source. Phys. Rev. Lett. 1997, 79, 233-236.
- [6] Shamrai, K.P. and Taranov, V.B. Resonance wave discharge and collisional energy absorption in helicon plasma source. Plasma Phys. Control Fusion 1994, 36, 1719-.
- [7] Blackwell, D.D., Madziwa, T.G., Arnush, D., and Chen, F.F. Evidence for Trivelpiece-Gould modes in a helicon discharge. Phys. Rev. Lett. 2002, 88, 145002-145005.
- [8] Krämer, M., Aliev, Yu. M., Altukhov, A.B., Gurchenko, A.D., Gusakov, E.Z., and Niemi, K. Anomalous helicon wave absorption and parametric excitation of electrostatic fluctuations in a helicon-produced plasma. Plasma Phys. Control. Fusion 2007, 49, A167-.
- [9] Boswell, R.W. and Chen, F.F. Helicons, the early years. IEEE Trans. Plasma Sci. 1997, 25, 1229-.
- [10] Chen, F.F. and Boswell, R.W. Helicons, the past decade. IEEE Trans. Plasma Sci. 1997, 25, 1245-.
- [11] Chen, F.F. Permanent magnet helicon source for ion propulsion. IEEE Trans. Plasma Sci. 2008, 36, 2095-2110.
- [12] Takahashi, K., Oguni, K., Uamada, H., and Fujiwara, T. Ion acceleration in a solenoid-free plasma expanded by permanent magnets. Phys. Plasmas 2008, 15, 084501-.
- [13] Curreli, D. and Chen, F.F. Equilibrium theory of cylindrical discharges with special application to helicons. Phys. Plasmas 2011, 18, 113501-
- [14] Chen, F.F. Physical mechanism of current-free double layers. Phys. Plasmas 2006, 13, 034502-.
- [15] Charles, C. Plasmas for spacecraft propulsion. J.Phys.D.Appl. Phys. 2009, 42, 163001-
- [16] Charles, C. A review of recent laboratory double layer experiments. Plasma Sources Sci. Technol. 2007, 16, R1-R
- [17] West, M.D., Charles, C., and Boswell, R.W. Testing a helicon double layer thruster immersed in a space-simulation chamber. J. Propul. and Power 2008, 24, 134-.
- [18] Crofton, M.W. and Pollard, J.E. Thrust augmentation by charge exchange. 49th AIAA/ASME/SAE/ASEE Joint Propulsion Conference, San Jose, CA, July 14-17, 2013; AIAA 2013-4131.
- [19] Takahashi, K, Lafleur, T., Charles, C., Alexander, P., Boswell, R. W., Perren, M., Laine, R., Pottinger, S., Lappas, V., Harle, T., and Lamprou, D. Direct thrust measurement of a permanent magnet helicon double layer thruster. Appl. Phys. Lett. 2011, 98, 141503-1 – 141503-3.
- [20] Takahashi, K., Lafleur, T., Charles, C., Alexander, P., and Boswell, R.W. Axial force imparted by a current-free magnetically expanding plasma. Phys. Plasmas 2012, 19, 083509-

- [21] Chen, F.F. and Torreblanca, H. Large-area helicon plasma source with permanent magnets, *Plasma Phys. Control. Fusion* 2007, 49, A81-
- [22] Chen, F.F. Performance of a permanent-magnet helicon source at 27 and 13 MHz, *Phys. Plasmas* 2012, 19, 093509-
- [23] Chang-Diaz, F.R. The VASIMR rocket. *Sci. Amer.* 2000, 283, No. 5, 90-
- [24] Squire, J.P., Chang-Diaz, F.R., Glover, T.W., Jacobson, V.T., McCaskill, G.E., Winter, D.S., Baity, F.W., Carter, M.D., and Goulding, R.H. High power light gas helicon plasma source for VASIMR. *Thin Solid Films* 2006, 506, 579-

## Bibliography

- Ahedo, E. and Navarro-Cavallé. Helicon thruster plasma modeling: Two-dimensional fluid-dynamics and propulsive performances. *Phys. Plasmas* 2013, 20, 043512-
- Ahedo, E. Plasmas for space propulsion. *Plasma Phys. Control. Fusion* 2011, 53, 124037-
- Biloiu, I.A. and Scime, E.E. Ion acceleration in Ar-Xe and Ar-He plasmas. II. Ion velocity distribution functions. *Phys. Plasmas* 2010, 17, 113509-
- Charles, C. Spatially resolved energy analyzer measurements of an ion beam on the low potential side of a current-free double-layer. *IEEE Trans. Plasma Sci.* 2005, 33, 336-
- Charles, C. and Boswell, R.W. The magnetic-field-induced transition from an expanding plasma to a double layer containing expanding plasma. *Appl. Phys. Lett.* 2007, 91, 201505-
- Charles C., Boswell, R., Alexander, P, Costa, C., Sutherland, O., Pfitzner, L., Franzen, R., Kingwell, J., Parfitt, A., Frigot, P.E., Del Amo, J., and Saccoccia G. Operating the helicon double layer thruster in a space simulation chamber. *IEEE Trans. Plasma Sci.* 2008, 36, 1196-
- Charles, C., Boswell, R.W. and Takahashi, K. Investigation of radiofrequency plasma sources for space travel. *Plasma Phys. Control. Fusion* 2012, 54, 124021-
- Charles, C., Boswell, R., and Takahashi, K. Boltzmann expansion in a radiofrequency conical helicon thruster operating in argon and xenon. *Appl. Phys. Lett.* 2013, 102, 223510-
- Corr, C.S. and Boswell, R.W. High-beta plasma effects in a low-pressure helicon plasma. *Phys. Plasmas* 2007, 14, 122503-
- Corr, C.S., Zanger, J., Boswell, R.W, and Charles, C. Ion beam formation in a low-pressure geometrically expanding argon plasma. *Appl. Phys. Lett.* 2007, 91, 241501-
- Corr, C.S., Boswell, R.W., Charles, C., and Zanger, J. Spatial evolution of an ion beam created by a geometrically expanding low-pressure argon plasma. *Appl. Phys. Lett.* 2008, 92, 221508-
- Cox, W., Hawkins, R., Charles, C., and Boswell, R. Three-dimensional mapping of ion density in a double-layer helicon plasma. *IEEE Trans. Plasma Sci.* 2008, 36, 1386-
- Cox, W., Charles, C., Boswell, R.W., and Hawkins, R. Spatial retarding field energy analyzer measurements downstream of a helicon double layer plasma. *Appl. Phys. Lett.* 2008, 93, 071505-
- Cox, W., West, M.K., Charles, C., *et al.* Three-dimensional magnetic field mapping of the magnetically steered helicon double-layer thruster. *IEEE Trans. Plasma Sci.* 2011, 39, 2160095-

- Giannelli, S., Kieckhafer, A., and Walker, M.L.R. Neutral gas expansion in a cylindrical helicon discharge chamber. *J. Propul. and Power* 2013, 29, 540-546.
- Harle, T., Pottinger, S.J., and Lappas, V.J. Helicon double layer thruster operation in a low magnetic field mode. *Plasma Sources Sci. Technol.* 2013, 22, 015015-
- Lafleur, T., Charles, C., and Boswell, R.W. Ion beam formation in a very low magnetic field expanding helicon discharge. *Phys. Plasmas* 2010, 17, 043505-
- Ling, J., West, M.D., Lafleur, T., Charles, C., and Boswell, R.W. Thrust measurements in a low-magnetic field high-density mode in the helicon double layer thruster. *J. Phys. D Appl. Phys.* 2010, 43, 305203-
- Plihon, N., Chabert, P., and Corr, C.S. Experimental investigation of double layers in expanding plasmas. *Phys. Plasmas* 2007, 14, 013506-
- Pottinger, S., Lappas, V., Charles, C., et al. Performance characterization of a helicon double layer thruster using direct thrust measurements. *J. Phys. D. Appl. Phys.* 2011, 44, 235201-
- Scime, E.E., Biloiu, I.A., Carr, J., Chakraborty, S., Thakur, M., Galante, A., Hansen, S., Houshmandyar, S., Keesee, A.M., McCarren, D., Sears, S., Biloiu, C., and Sun, X. Time-resolved measurements of double layer evolution in expanding plasma. *Phys. Plasmas* 2010, 17, 055701-
- Sun, X., Keesee, A.M., Biloiu, C., and Scime, E.E. Observations of ion-beam formation in a current-free double layer. *Phys. Rev. Lett.* 2005, 95, 025004-
- Sutherland, O., Charles, C., Plihon, N., and Boswell, R.W. Experimental evidence of a double layer in a large volume helicon reactor. *Phys. Rev. Lett.* 2005, 95, 205002-
- Takahashi, K., Charles, C., Boswell, R.W., Kaneko, T., and Hatakeyama, R. Measurement of the energy distribution of trapped and free electrons in a current-free double layer. *Phys. Plasmas* 2007, 14, 114503-
- Takahashi, K. and Fujiwara, T. Observation of weakly and strongly diverging ion beams in a magnetically expanding plasma. *Appl. Phys. Lett.* 2009, 94, 061502-
- Takahashi, K., Igarashi, Y., and Fujiwara, T. Plane and hemispherical potential structures in magnetically expanding plasmas. *Appl. Phys. Lett.* 2010, 97, 041501-
- Takahashi, K., Charles, C., and Boswell, R.W. Approaching the theoretical limit of diamagnetic-induced momentum in a rapidly diverging magnetic nozzle. *Phys. Rev. Lett.* 2013, 110, 195003-
- West, M.D., Charles, C., and Boswell, R.W. Mode transitions in the helicon double layer thruster prototype operating in xenon. *IEEE Trans. Plasma Sci.* 2011, 39, 2468-
- Williams, L.T., and Walker, M.L.R. Thrust measurements of a radio frequency plasma source. *J. Propul. and Power* 2013, 29, 520-527.

## Figures

Fig. 1. Schematic of a gridded ion thruster.

Fig. 2. Schematic of a Hall thruster

Fig. 3. Diagram of ion and electron densities in a Debye sheath.

Fig. 4 Schematic of diverging field lines from a helicon source.

Fig. 5. Generic schematic of a helicon thruster.

Fig. 6. Schematic of a permanent-magnet helicon thruster with ring magnets, showing placement of the discharge in the remote field [21].

Fig. 7. Schematic of a permanent-magnet helicon thruster with linear magnets. Courtesy of K. Takahashi [12].

**Figure 1**

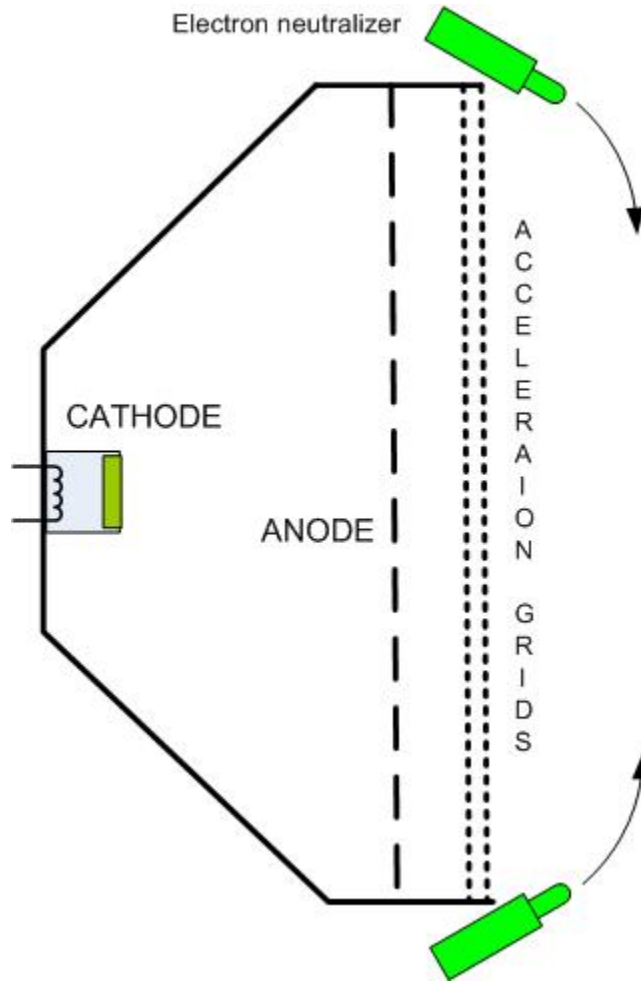
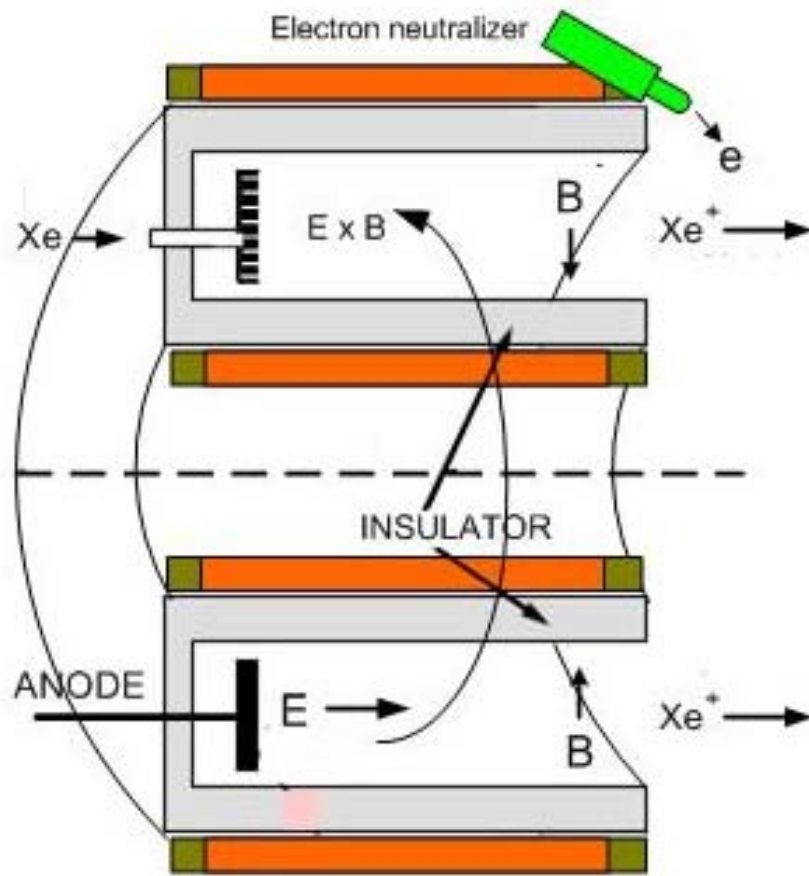
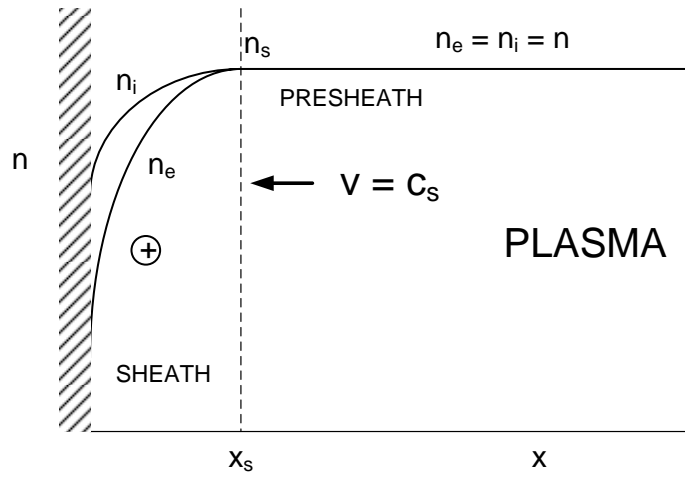


Figure 2



**Figure 3**



**Figure 4**

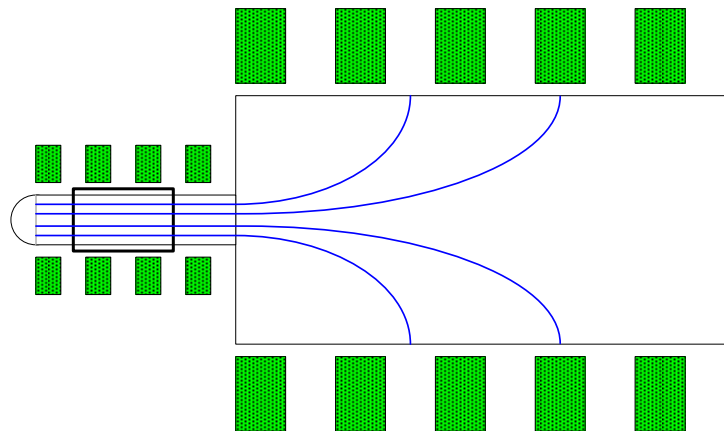
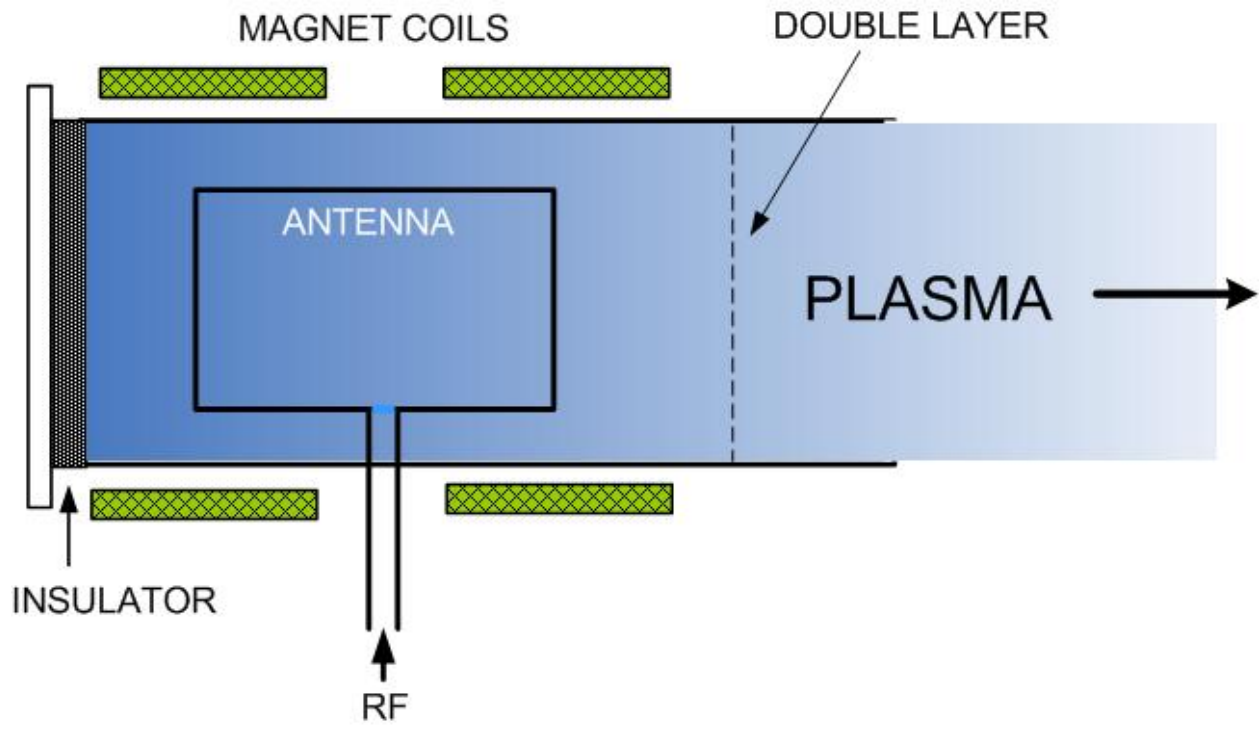
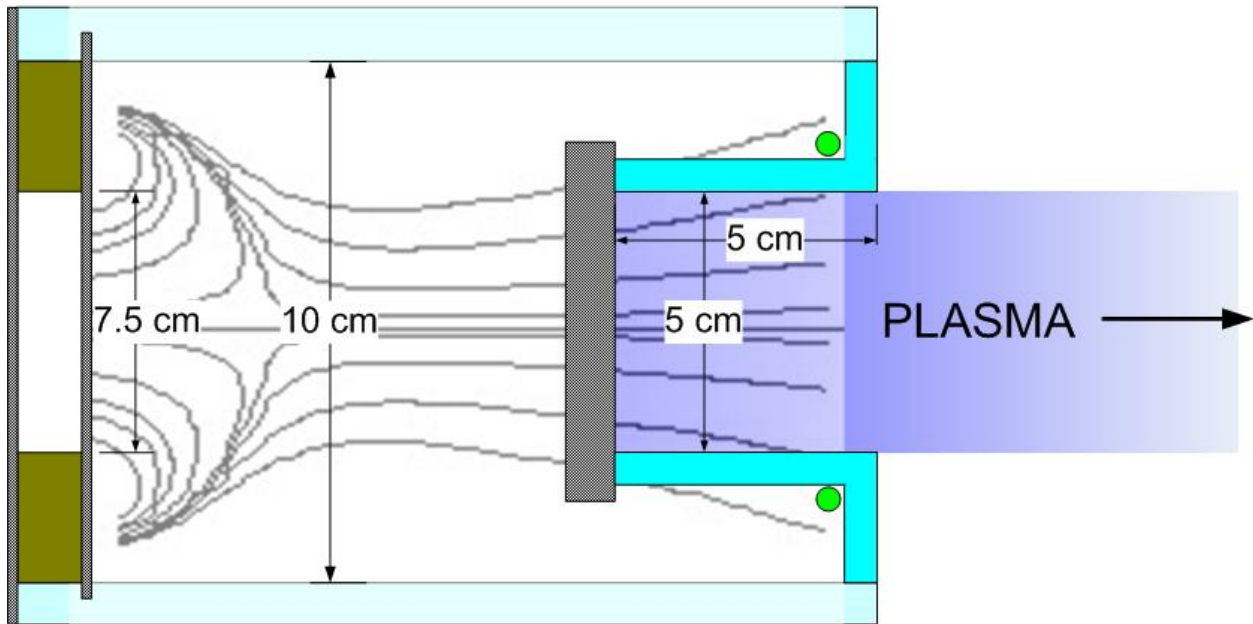


Figure 5





**Figure 6**



**Figure 7**

